Prevention of hepatic steatosis and hepatic insulin resistance in mitochondrial acyl-CoA:glycerol-sn-3-phosphate acyltransferase 1 knockout mice

Susanne Neschen,[1,2] Katsutaro Morino,[1,2] Linda E. Hammond,[3] Dongyan Zhang,[2] Zhen-Xiang Liu,[2] Anthony J. Romanelli,[2] Gary W. Cline,[2] Rebecca L. Pongratz,[2] Xian-Man Zhang,[2] Cheol S. Choi,[2] Rosalind A. Coleman,[3] and Gerald I. Shulman[1,2,*]

[1]Howard Hughes Medical Institute
[2]Departments of Internal Medicine and Cellular & Molecular Physiology, Yale University School of Medicine, New Haven, Connecticut 06520
[3]Department of Nutrition, University of North Carolina, Chapel Hill, North Carolina
*Correspondence: gerald.shulman@yale.edu

Summary

In order to investigate the role of mitochondrial acyl-CoA:glycerol-sn-3-phosphate acyltransferase 1 (mtGPAT1) in the pathogenesis of hepatic steatosis and hepatic insulin resistance, we examined whole-body insulin action in awake *mtGPAT1* knockout (*mtGPAT1*$^{-/-}$) and wild-type (wt) mice after regular control diet or three weeks of high-fat feeding. In contrast to high-fat-fed wt mice, *mtGPAT1*$^{-/-}$ mice displayed markedly lower hepatic triacylglycerol and diacylglycerol concentrations and were protected from hepatic insulin resistance possibly due to a lower diacylglycerol-mediated PKCϵ activation. Hepatic acyl-CoA has previously been implicated in the pathogenesis of insulin resistance. Surprisingly, compared to wt mice, *mtGPAT1*$^{-/-}$ mice exhibited increased hepatic insulin sensitivity despite an almost 2-fold elevation in hepatic acyl-CoA content. These data suggest that mtGPAT1 might serve as a novel target for treatment of hepatic steatosis and hepatic insulin resistance and that long chain acyl-CoA's do not mediate fat-induced hepatic insulin resistance in this model.

Introduction

Concurrent with the existing epidemic of obesity, hepatic steatosis is rapidly becoming a major health care problem. Hepatic steatosis is associated with altered liver function, hyperlipidemia, and progression to liver cirrhosis (Lee, 1989; Marchesini et al., 1999). Furthermore recent studies have demonstrated an important role of hepatic steatosis in the pathogenesis of hepatic insulin resistance, increased hepatic gluconeogenesis, and fasting hyperglycemia in patients with type 2 diabetes (Mayerson et al., 2002, Petersen et al., 2005; Petersen et al., 2002; Pietilainen et al., 2005). Understanding the steps involved in the regulation of hepatic triacylglycerol synthesis might be expected to yield important new information regarding the pathogenesis of nonalcoholic fatty liver disease (NALFD) and hepatic insulin resistance as well as providing potential novel targets for their treatment and prevention.

In this context, we examined whether or not a mouse model deficient in the mitochondrial isoform of acyl-CoA:glycerol-sn-3-phosphate acyltransferase 1 (mtGPAT1) would be protected from fat-induced hepatic steatosis and hepatic insulin resistance. GPAT has been hypothesized to control the rate-controlling step in the glycerol 3-phosphate pathway, catalyzing the acylation of glycerol-3-phosphate with acyl-coenzyme A (CoA) generating CoA and 1-acyl-*sn*-glycerol 3-phosphate (lysophosphatidic acid, Figure 1). Three different isoenzymes of GPAT have been described to date, one located in the endoplasmic reticulum (msGPAT) and two in the outer mitochondrial membrane (mtGPAT1 and mtGPAT2; Bhat et al., 1999; Coleman and Haynes, 1983; Coleman and Lee, 2004; Lewin et al., 2004; Monroy et al., 1972; Shin et al., 1991). Among these three isoforms only *mtGPAT1* has been sequenced (Bhat et al., 1999; Paulauskis and Sul, 1988; Shin et al., 1991; Yet et al., 1993).

Previous in vitro studies have demonstrated that overexpression of *mtGPAT* in cell cultures primarily results in the trafficking of exogenous fatty acids into the triacylglycerol pool rather than incorporation into phospholipid fractions or into oxidative degradation (Igal et al., 2001; Lindén et al., 2004). Thus, it has been proposed that the mitochondrial mtGPAT1 isoform might serve as a valve that channels fatty-acid derivatives preferentially toward glycerolipid synthesis, counteracting their partitioning into the β-oxidation pathway (Lewin et al., 2005; Hammond et al., 2002).

The glycerol-3-phosphate pathway provides lipid metabolites, such as acyl-CoA, lysophosphatidic acid, diacylglycerol, and triacylglycerol (Figure 1), which have all been suggested to play a role in the development of insulin resistance (Griffin et al., 1999; Jucker et al., 1999; Kraegen et al., 2001; Neschen et al., 2002; Samuel et al., 2004; Shulman, 2000; Yu et al., 2002). Since liver is among the organs displaying the highest specific mtGPAT enzyme activity, we surmised that systemic *mtGPAT1* deletion in mice would affect acyl-CoA, lysophosphatidic acid, diacylglycerol, and triacylglycerol abundance predominantly in the liver and that these alterations in lipid metabolites might provide some novel insights into the pathogenesis of hepatic steatosis and hepatic insulin resistance.

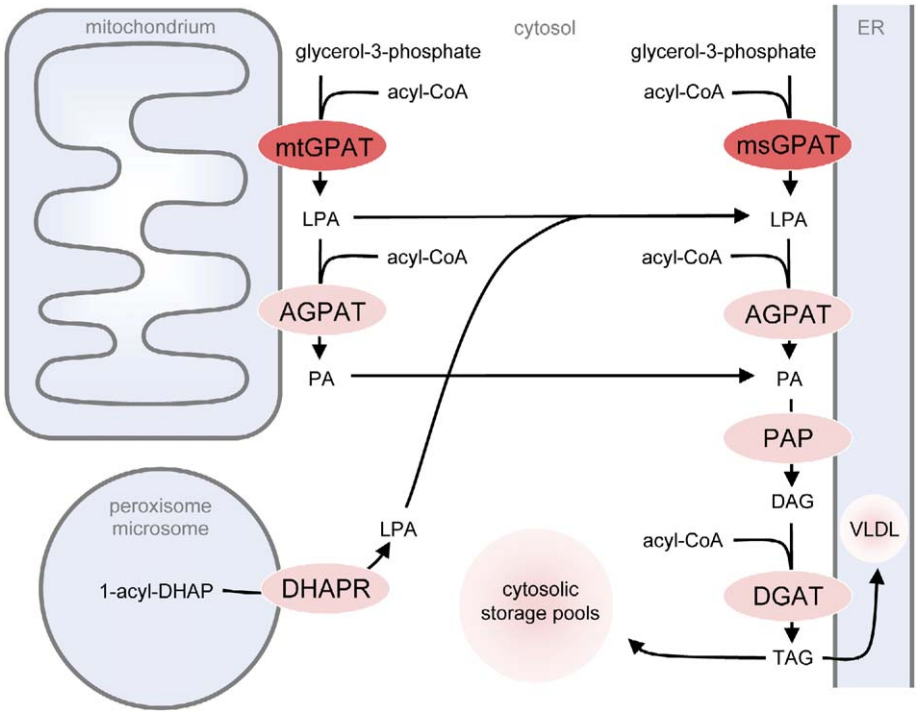

Figure 1. Glycerol-3-phosphate pathway

The glycerol 3-phosphate or phosphatidic acid pathway represents the de novo route in the synthesis of triacylglycerol (TAG) and phospholipids. acyl-CoA:glycerol-sn-3-phosphate acyltransferase (GPAT) catalyzes the acylation of sn-glycerol-3-phosphate with acyl-coenzyme A (acyl-CoA) generating lysophosphatidic acid (LPA), which is thought to be the rate-controlling step in triglyceride synthesis. Subsequent reactions are catalyzed by acyl-CoA:1-acylglycerol-sn-3-phosphate acyltransferase (AGPAT), phosphatidic acid phosphatase (PAP), and diacylglycerol:acyl-CoA acyltransferase (DGAT) isoenzymes generating phosphatidic acid (PA), diacylglycerol (DAG), and triacylglycerol (TAG). In liver, triacylglycerol is either deposited in intracellular lipid vacuoles or exported in very low-density lipoprotein (VLDL) particles. Lysophosphatidic and phosphatidic acid generated at cell organelles other than the endoplasmic reticulum require translocation through the cytosol for triacylglycerol synthesis at the endoplasmic reticulum (modified from Coleman and Lee, 2004).

Results

Metabolic phenotype and glucose tolerance in regular chow- and high-fat-diet-fed *mtGPAT1*$^{-/-}$ and wt mice

To evaluate the effect of *mtGPAT1* deletion on whole-body physiology, we assessed food intake, fat absorption, body weight, whole body fat content, as well as plasma metabolite and hormone concentrations from *mtGPAT1*$^{-/-}$ and wt mice fed a control diet or a high-fat diet for three weeks (Table 1). Body weights and plasma concentrations of glucose, fatty acids, insulin, glucagon, adiponectin, and leptin did not differ among *mtGPAT1*$^{-/-}$ and wt mice fed the control diet. In contrast, plasma triacylglycerol concentrations and whole-body fat mass were ~30% and ~20% lower in *mtGPAT1*$^{-/-}$ mice compared to the wt mice (Table 1).

When the control diet was changed to a high-fat diet, *mtGPAT1*$^{-/-}$ mice consumed a higher amount of dietary calories but also absorbed less fat from the diet than wt mice, resulting in an overall similar weight gain. Plasma concentrations of glucose, fatty acids, insulin, glucagon, corticosterone, resistin, adiponectin, and leptin did not differ among *mtGPAT1*$^{-/-}$ and wt mice after 3 weeks of high-fat feeding, but plasma triglycerides were 30% lower in the *mtGPAT1*$^{-/-}$ mice (Table 1).

When fed a control diet, *mtGPAT1*$^{-/-}$ and wt mice displayed similar plasma-glucose and insulin responses following an intraperitoneal glucose challenge (Figures 2A and 2C). Following only one week of high-fat feeding, *mtGPAT1*$^{-/-}$ mice displayed a markedly improved glucose tolerance compared to wt mice (Figures 2B and 2D).

Hyperinsulinemia (197 ± 22, n = 7 versus 176 ± 25, n = 7 μU/ml insulin in wt) in response to an intraperitoneal insulin injection decreased plasma fatty acid (0.42 ± 0.03, n = 7 versus 0.48 ± 0.04, n = 7 mmol/l nonesterified fatty acids in wt) and triacylglycerol (53 ± 4, n = 7 versus 67 ± 6, n = 7 mmol/l triacylglycerol in wt) concentrations to a comparable extent in high-fat-diet-fed *mtGPAT1*$^{-/-}$ and wt mice. Under hyperinsulinemic conditions, plasma resistin (4.9 ± 0.7, n = 4 versus 4.8 ± 0.7, n = 3 ng/ml in wt) and β-hydroxybutyrate levels did not differ between genotypes (0.36 ± 0.14, n = 5 versus 0.43 ± 0.06, n = 4 β-hydroxybutyrate in wt). Relative to the fasting state, β-hydroxybutyrate concentrations declined more than 4-fold with insulin stimulation in *mtGPAT1*$^{-/-}$ compared to only 2-fold in high-fat-diet-fed wt mice (Table 1).

Improved insulin sensitivity in high-fat-diet-fed *mtGPAT1*$^{-/-}$ mice is due to preservation of hepatic insulin sensitivity

Euglycemic-hyperinsulinemic clamp experiments confirmed no genotypic differences in whole-body- and organ-specific insulin sensitivity reflected by comparable glucose infusion rates (Figure 3A), peripheral insulin sensitivity (Figure 3C), and hepatic insulin sensitivity (Figure 3E).

In contrast, when euglycemic-hyperinsulinemic clamp studies were performed after three weeks of high-fat diet feeding, *mtGPAT1*$^{-/-}$ mice showed increased insulin sensitivity compared to wt mice as reflected by a 40% higher glucose infusion rate required to maintain euglycemia than in wt mice (Figure 3B). Improved insulin sensitivity in high-fat-diet-fed *mtGPAT1*$^{-/-}$ compared to wt mice could almost entirely be attributed to increased hepatic insulin sensitivity. The decline in hepatic insulin sensitivity observed in wt mice fed the high-fat diet was completely rescued by *mtGPAT1* deletion, and insulin suppressed hepatic glucose production by almost 80% in high-fat-fed versus 82% in control-diet-fed *mtGPAT1*$^{-/-}$ mice (Fig-

Table 1. Physiologic and plasma parameters in wt and *mtGPAT1*$^{-/-}$ mice

	Control diet		High-fat diet	
	wt	*mtGPAT1*$^{-/-}$	wt	*mtGPAT1*$^{-/-}$
Physiologic parameters				
Body weight (g)	27.3 ± 0.3 (n = 25)	27.0 ± 0.4 (n = 22)	29.3 ± 0.5 (n = 25)	28.4 ± 0.5 (n = 22)
Whole-body fat content (%BW)	8.0 ± 0.5 (n = 25)	6.5 ± 0.6* (n = 22)	14.8 ± 0.9 (n = 25)	12.8 ± 0.7 (n = 22)
Whole-body fat gain (%BW/3 weeks)	—	—	6.8 ± 0.9 (n = 25)	6.3 ± 0.7 (n = 22)
Calorie consumption (kcal/day/g BW)	0.52 ± 0.02 (n = 3)	0.47 ± 0.01 (n = 3)	0.48 ± 0.01 (n = 20)	0.51 ± 0.01* (n = 18)
Fat absorption (% linoleic acid)	99.4 ± 0.2 (n = 5)	98.1 ± 1.0 (n = 5)	99.4 ± 0.2 (n = 5)	97.5 ± 0.4* (n = 5)
Plasma metabolites				
Glucose (mg/dl)	147 ± 6 (n = 11)	148 ± 5 (n = 11)	142 ± 7 (n = 13)	143 ± 6 (n = 11)
Total cholesterol (mg/dl)	82 ± 7 (n = 5)	75 ± 3 (n = 5)	103 ± 8 (n = 13)	88 ± 5 (n = 11)
HDL cholesterol (mg/dl)	67 ± 4 (n = 5)	61 ± 2 (n = 5)	78 ± 5 (n = 13)	67 ± 4 (n = 11)
Triacylglycerol (mmol/l)	89 ± 5 (n = 5)	64 ± 3* (n = 5)	121 ± 12 (n = 9)	88 ± 8* (n = 10)
Nonesterified fatty acid (meq/l)	0.74 ± 0.07 (n = 5)	0.70 ± 0.04 (n = 5)	0.83 ± 0.10 (n = 13)	0.73 ± 0.08 (n = 11)
β-hydroxybutyrate (mmol/l)	1.1 ± 0.2 (n = 5)	1.2 ± 0.1 (n = 5)	0.94 ± 0.09 (n = 9)	1.55 ± 0.36* (n = 7)
Plasma hormones and adipocyte cytokines				
Insulin (μU/ml)	15 ± 1 (n = 6)	16 ± 1 (n = 6)	19 ± 1 (n = 13)	17 ± 2 (n = 11)
Glucagon (pg/ml)	n.d.	n.d.	64 ± 4 (n = 7)	62 ± 5 (n = 5)
Corticosterone (ng/ml)	n.d.	n.d.	61 ± 14 (n = 13)	65 ± 9 (n = 11)
Resistin (ng/ml)	n.d.	n.d.	3.8 ± 0.2 (n = 9)	3.8 ± 0.3 (n = 10)
Adiponectin (μg/ml)	19 ± 7 (n = 2)	15 ± 1 (n = 2)	15 ± 1 (n = 13)	15 ± 1 (n = 11)
Leptin (ng/ml)	6.9 ± 0.1 (n = 2)	6.9 ± 1.4 (n = 2)	7.2 ± 1.1 (n = 11)	5.5 ± 0.4 (n = 9)

Physiologic and plasma parameters were determined throughout control diet or at the end of 3 weeks of high-fat diet feeding (*p < 0.05; **p < 0.001; n.d., not determined).

ures 3E and 3F). In contrast, in wt mice, high-fat diet feeding completely abolished insulin's ability to suppress hepatic glucose production (Figure 3F).

Enhanced hepatic insulin sensitivity in high-fat-fed *mtGPAT1*$^{-/-}$ mice after short-term insulin exposure was associated with a 1.3-fold increased insulin-receptor substrate 2-associated phosphatidyl inositol-3-kinase activity (PI3K, Figure 4D) and a 1.4-fold increased Akt2 activity (Figure 4E) in liver. The activation of PKCε has recently been implicated in high-fat-diet-induced hepatic insulin resistance in rats (Samuel et al., 2004). Hepatic PKCε activity, as reflected by the ratio of PKCε in cellular membranes and the cytosolic fraction, was markedly decreased in the livers of high-fat-fed *mtGPAT1*$^{-/-}$ mice compared to the wt mice (Figure 4C).

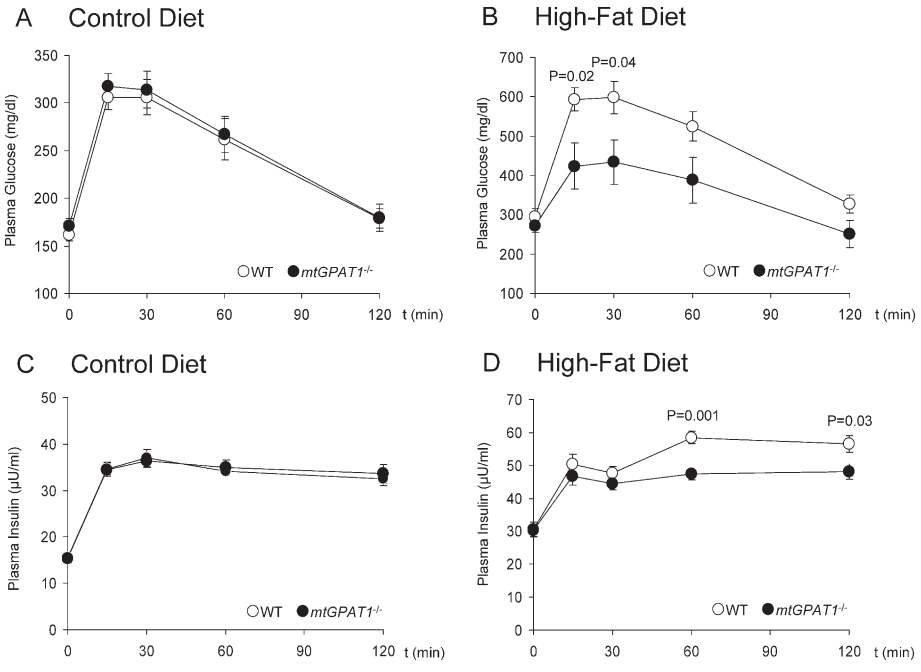

Figure 2. Intraperitoneal glucose tolerance tests

Experiments were performed in wt and *mtGPAT1*$^{-/-}$ mice fed either a control diet or high-fat diet for 1 week. For (**A** and **B**) plasma-glucose and (**C** and **D**) insulin measurements, a basal blood sample was obtained at minute 0 from fasting (control diet 16 hr, high-fat diet 7 hr) mice and additional blood samples after injection of 1 g glucose/kg BW at minutes 15, 30, 60, and 120. Results are expressed as means ± SEM (n = 7–9).

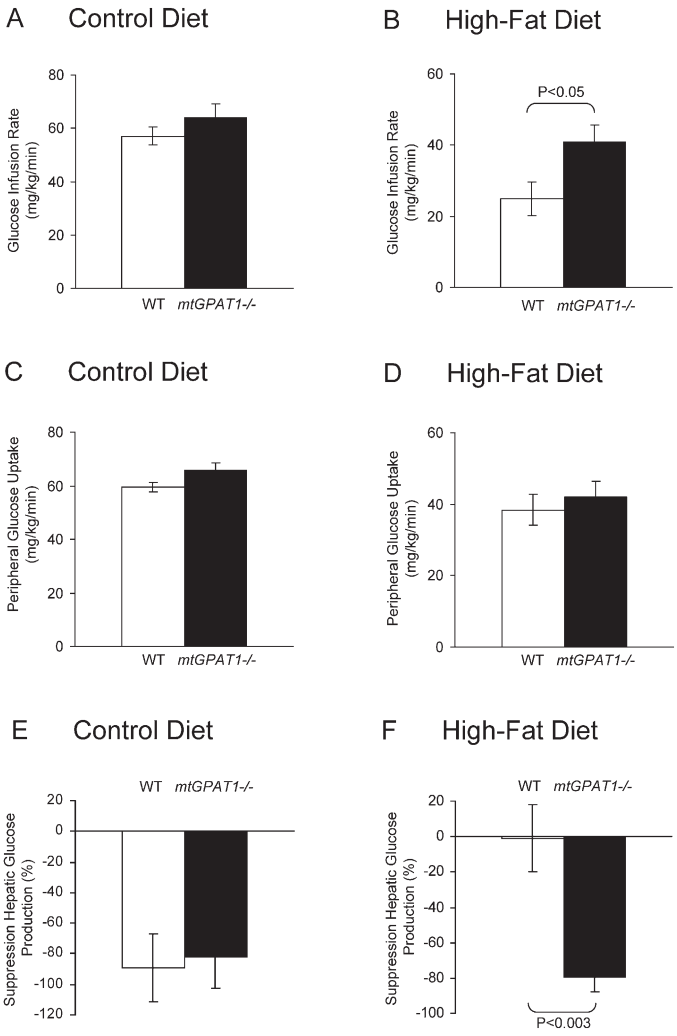

Figure 3. Euglycemic-hyperinsulinemic clamp experiments

wt and *mtGPAT1*$^{-/-}$ mice fed a control diet or a high-fat diet for 3 weeks were 16 hr food-deprived prior to euglycemic-hyperinsulinemic (2.5 mU/kg/min) clamp experiments. Plasma glucose under hyperinsulinemic conditions was maintained by an intravenous variable 20% glucose infusion, and rates of (**A** and **B**) glucose infusion, (**C** and **D**) peripheral glucose uptake, and (**E** and **F**) insulin-mediated suppression of hepatic glucose production were determined under steady-state conditions. Results are expressed as means ± SEM (n = 4–5 control diet, n = 7–8 high-fat diet).

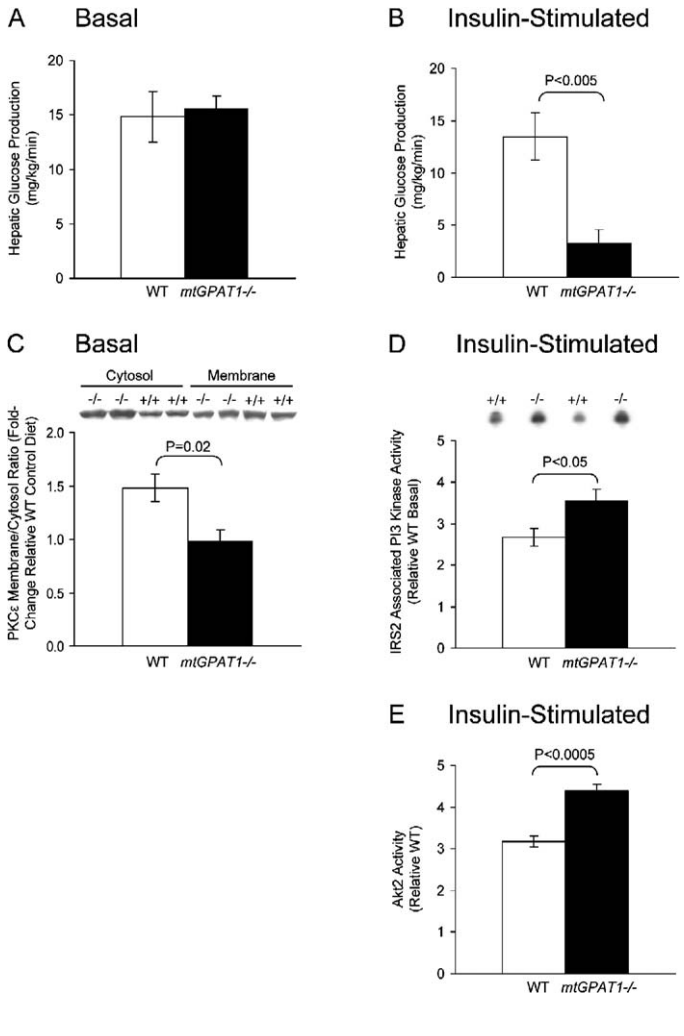

Figure 4. Hepatic insulin sensitivity and hepatic insulin signaling

Hepatic glucose production in wt and *mtGPAT1*$^{-/-}$ mice fed a high-fat diet for 3 weeks was determined under (**A**) basal and (**B**) insulin-stimulated conditions in euglycemic-hyperinsulinemic (2.5 mU/kg/min) clamp experiments. (**C**) Immunoblots determining membrane and cytosolic PKCε content were performed with liver protein extracts from fasting high-fat-diet-fed mice. (**D** and **E**) Kinase assays were performed with liver protein extracts obtained from fasted, high-fat-fed mice 20 min after an intraperitoneal insulin injection (0.5 mU/kg). Results are expressed as means ± SEM (n = 6–8).

Despite no evidence for a genotypic difference in the expression of the gluconeogenic enzyme PEPCK under insulin-stimulated conditions (100 ± 11, n = 9 versus 108 ± 11, n = 9% copies/18S rRNA in wt), insulin increased SREBP-1c gene expression 1.5-fold in high-fat-diet-fed *mtGPAT1*$^{-/-}$ relative to wt mice (100 ± 11, n = 8 versus 169 ± 12, n = 8% copies/18S rRNA in wt), whereas under fasting conditions, SREBP-1c gene expression was unaltered (100 ± 14, n = 8 versus 116 ± 11, n = 8% copies/18S rRNA in wt).

There was no effect of systemic *mtGPAT1* deletion on peripheral glucose utilization (Figure 3D) and insulin-stimulated 2-[^{14}C]DG uptake in gastrocnemii muscles (299 ± 50, n = 6 versus 298 ± 33, n = 8 nmol/g skeletal muscle/min glucose in wt). White adipose tissue, which also displays high mtGPAT activity, had an ~30% increase in insulin-stimulated 2-[^{14}C]DG uptake in *mtGPAT1*$^{-/-}$ compared to wt mice (108 ± 14, n = 7 versus 72 ± 5, n = 8 nmol/g adipose tissue/min glucose in wt, $p < 0.03$).

Improved hepatic insulin sensitivity in high-fat-diet-fed *mtGPAT1*$^{-/-}$ mice is associated with decreased lysophosphatidic acid, diacylglycerol, and triacylglycerol content but increased acyl-CoA content

Deletion of mtGPAT1 limited the acylation of glycerol-3-phosphate, resulting in a 1.6-fold increase in the intrahepatic acyl-CoA pool in the high-fat-diet *mtGPAT1*$^{-/-}$ relative to wt mice (Table 2; Figure 5A). In addition, insulin stimulation caused a further 2.7-fold increase in acyl-CoA in high-fat-diet-fed *mtGPAT1*$^{-/-}$ compared to wt mice (624.5 ± 52.1, n = 7 versus

Table 2. Tissue lipid metabolites from high-fat-diet-fed fasting wt and *mtGPAT1*$^{-/-}$ mice

	wt	*mtGPAT1*$^{-/-}$
Total liver lipid metabolites		
Acyl-CoA (nmol/g liver)	631.9 ± 33.5 (n = 7)	1038.4 ± 56.0*** (n = 7)
Lysophosphatidic acid (nmol/g liver)	3.9 ± 0.1 (n = 5)	0.6 ± 0.0*** (n = 6)
Phosphatidic acid (nmol/g liver)	11.9 ± 0.3 (n = 5)	11.2 ± 0.4 (n = 6)
Diacylglycerol (μmol/g liver)	3.27 ± 0.42 (n = 7)	1.43 ± 0.14** (n = 6)
Triacylglycerol (μmol/g liver)	53.6 ± 4.3 (n = 15)	35.8 ± 2.0** (n = 15)
Total skeletal muscle metabolites		
Acyl-CoA (nmol/g muscle)	30.5 ± 6.5 (n = 7)	31.2 ± 5.7 (n = 5)
Triacylglycerol (μmol/g muscle)	12.9 ± 3.6 (n = 7)	12.8 ± 3.2 (n = 7)

Lipid metabolites were extracted from freeze-clamped livers and gastrocnemii muscles obtained from fasting wt and *mtGPAT1*$^{-/-}$ mice after 3 weeks of high-fat-diet feeding. Total acyl-CoA, lysophosphatidic acid, and diacylglycerol concentrations are given as the sum of the individual metabolite species (*$p < 0.03$; **$p < 0.005$; ***$p < 0.00005$).

234.6 ± 26.6, n = 7 nmol/g liver total post-clamp acyl-CoA in wt, $p < 0.0001$).

Under fasting conditions, total hepatic lysophosphatidic acid content was markedly reduced in high-fat-diet-fed *mtGPAT1*$^{-/-}$ compared to wt mice (Table 2; Figure 5B). Intracellular lysophosphatidic acid abundance has been connected to phosphorylation and activation of glycogen synthase kinase 3 (pGSK-3) in the past. In the presence of decreased lysophosphatidic acid levels, the hepatic pGSK-3 content tended to be lower in fasting high-fat-diet-fed *mtGPAT1*$^{-/-}$ than in wt mice (2.2 ± 0.5, n = 7 versus 1.6 ± 0.3, n = 7 fold-change in pGSK-3 relative to control diet). Insulin markedly elevated total hepatic LPA content (13.2 ± 2.5, n = 3 versus 4.1 ± 0.3, n = 6 nmol/g liver total post-clamp LPA in wt) in *mtGPAT1*$^{-/-}$ mice, affecting the majority of measured species to a similar extent (data not shown). Total hepatic phosphatidic acid content as well as all individual phosphatidic acid species (data not shown) showed no genotypic differences in high-fat-diet-fed mice (Table 2).

Total hepatic diacylglycerol content as well as various individual diacylglycerol species were markedly reduced in livers of high-fat-diet-fed *mtGPAT1*$^{-/-}$ compared to wt mice (Table 2; Figure 5C). No marked genotypic differences were evident when the control diet was fed to *mtGPAT1*$^{-/-}$ and wt mice (data not shown).

When fed the control diet, *mtGPAT1*$^{-/-}$ mice displayed a markedly lower hepatic triacylglycerol content (4.0 ± 0.5, n = 5 versus 8.8 ± 1.7, n = 5 μmol/g liver triacylglycerol, p = 0.02). High-fat feeding raised hepatic triacylglycerol concentrations

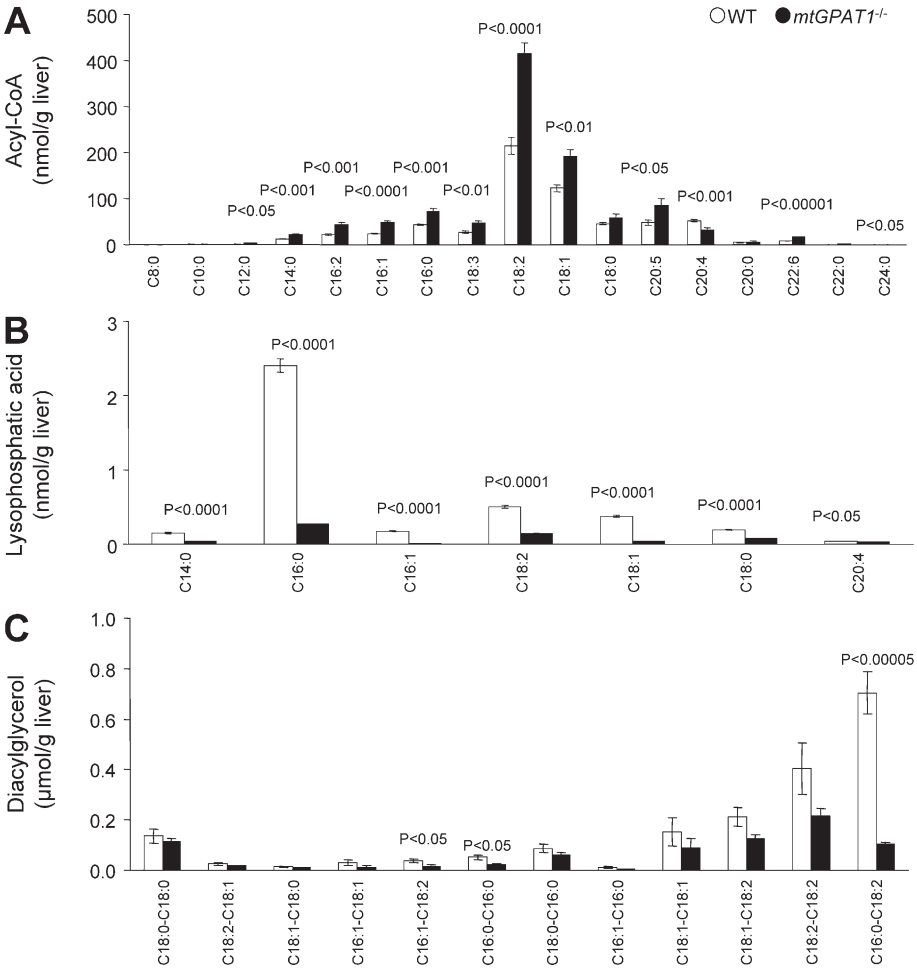

Figure 5. Hepatic lipid metabolite profiles

(**A**) acyl-CoA, (**B**) lysophosphatidic acid, and (**C**) diacylglycerol species (depicts only a fraction of measured species) were extracted from livers of fasting wt and *mtGPAT1*$^{-/-}$ mice fed a high-fat diet for 3 weeks. Species were measured with an API 3000 tandem mass spectrometer interfaced with a turbo ionspray source in negative electrospray mode. Results are expressed as means ± SEM (n = 7–8).

7- and 10-fold in wt and *mtGPAT1*$^{-/-}$ mice, but the total hepatic triacylglycerol content in *mtGPAT1*$^{-/-}$ mice remained significantly below that measured in wt mice (Table 2).

The absence of *mtGPAT1* in mice did not alter the acyl-CoA or triacylglycerol concentrations in skeletal muscle with high-fat-diet feeding (Table 2).

Hepatic pAMPK protein content, pACC protein content, and malonyl-CoA levels are not altered in livers of high-fat-diet-fed *mtGPAT1*$^{-/-}$ mice

A 40% increase in fasting plasma β-hydroxybutyrate concentrations (Table 1) in high-fat-diet-fed *mtGPAT1*$^{-/-}$ mice likely reflected higher rates of hepatic fatty-acid β-oxidation and thus we assessed key regulatory mechanisms of fatty-acid β-oxidation in liver. The hepatic protein content of phosphorylated AMP-activated protein kinase (Supplemental data available with this article online), phosphorylated acetyl-CoA carboxylase (Supplemental data), and hepatic malonyl-CoA (2.3 ± 0.8, n = 4 versus 2.4 ± 0.6, n = 3 nmol/g liver malonyl-CoA in wt) were comparable in the *mtGPAT1*$^{-/-}$ and wt genotypes. Despite marked increases of n-3 fatty-acid derivatives in livers of *mtGPAT1*$^{-/-}$ mice (Figure 5A), neither the expression of PPARα (100 ± 11, n = 9 versus 88 ± 11, n = 9% copies/18S rRNA in wt) nor the PPARα-responsive gene peroxisomal acyl-CoA oxidase 1 (100 ± 11, n = 9 versus 114 ± 11, n = 9% copies/18S rRNA in wt) differed between genotypes. The hepatic expression of the VLCAD gene (100 ± 13, n = 6 versus 114 ± 14, n = 6% copies/18S rRNA in wt) and the LCAD gene (100 ± 11, n = 9 versus 102 ± 11, n = 9% copies/18S rRNA in wt), both involved in fatty-acid β-oxidation, were similar in high-fat-fed *mtGPAT1*$^{-/-}$ and wt mice.

Discussion

Here we show that systemic *mtGPAT1* deletion substantially limits the incorporation of acyl-CoA species into the sn-glycerol 3-phosphate pathway in liver resulting in markedly lower hepatic triacylglycerol but higher acyl-CoA abundance and increased plasma β-hydroxybutyrate concentrations, most likely as a result of increased hepatic ketogenesis. Therefore, the two alternative GPAT isoforms mtGPAT2 and msGPAT appear to be incapable of compensating for mtGPAT1 in liver.

Surprisingly, systemic deletion of *mtGPAT1* completely protected mice from developing high-fat-diet-induced hepatic insulin resistance despite a large increase in hepatic acyl-CoA content. Improved hepatic insulin action in *mtGPAT1*$^{-/-}$ mice was also evident in enhanced hepatic insulin signaling, transcriptional induction of the insulin-responsive gene SREBP-1c, and a pronounced insulin-mediated decline in plasma β-hydroxybutyrate levels, the latter likely the result of an enhanced insulin-mediated suppression of hepatic ketogenesis. The fact that increased tissue-specific insulin sensitivity in high-fat-fed *mtGPAT1*$^{-/-}$ mice was exclusively evident in liver and white adipose tissue but not skeletal muscle is consistent with the enzyme's tissue-specific activity pattern. In rat it has been reported that in the majority of tissues, including skeletal muscle, mtGPAT comprises only 10% of total GPAT enzyme activity whereas in liver and white adipose tissue mtGPAT can comprise up to 50% of total GPAT enzyme activity (Coleman et al., 2000; Lewin et al., 2001). The improved hepatic insulin sensitivity in *mtGPAT1*$^{-/-}$ mice was not mediated by changes in major circulating adipocyte cytokines as plasma leptin, adiponectin, and resistin concentrations were unchanged.

Previous studies have linked the accumulation of various lipid metabolites, such as acyl-CoA species, lysophosphatidic acid, diacylglycerol, or triacylglycerol in liver and skeletal muscle with the pathogenesis of insulin resistance (Chen et al., 1992; Griffin et al., 1999; Hegarty et al., 2003; Jucker et al., 1999; Kraegen et al., 2001; Petersen et al., 2004; Samuel et al., 2004; Shulman, 2000; Yu et al., 2002). As demonstrated in this study, systemic deletion of *mtGPAT1* affects the abundance of lipid metabolites primarily in the liver, and the absence of major physiologic and metabolic changes makes this an ideal model to study the role of an array of lipid candidates in the genesis of hepatic insulin resistance.

An important finding in the current study is that despite an almost 2-fold increase in the abundance of long-chain and very long-chain acyl-CoA species in the liver, high-fat-diet-fed mtGPAT1$^{-/-}$ mice were protected from fat-induced hepatic insulin resistance, providing strong evidence against a role of acyl-CoA species in mediating this pathologic process.

A role of lysophosphatidic acid as a mediator of insulin resistance has also been suggested in the past. Systemic deletion of *mtGPAT1* resulted in a very pronounced reduction of hepatic lysophosphatidic acid concentrations under fasting conditions and was accompanied by a tendency for a lower hepatic pGSK-3 protein content in *mtGPAT1*$^{-/-}$ mice. Lysophosphatidic acid has been shown to be capable of inducing the phosphorylation and activation of the serine/threonine kinase GSK-3 primarily via a protein kinase C-dependent pathway and thereby could interfere with insulin signaling (Fang et al., 2002). Surprisingly, insulin stimulation markedly raised hepatic lysophosphatidic acid content in *mtGPAT1*$^{-/-}$ compared to wt mice. Since *mtGPAT1*$^{-/-}$ mice were protected from fat-induced hepatic insulin resistance, these data argue against a major role for lysophosphatidic acid in mediating fat-induced hepatic insulin resistance. The fact that C16:0 lysophosphatidic acid dominated the spectrum suggests that the majority of hepatic lysophosphatidic acid was not directly synthesized from dietary C18:2n-6, the most abundant fatty-acid species in safflower oil. It rather appears that lysophosphatidic acid was mainly derived from de novo lipogenesis and/or from induction of phospholipase A by insulin (Shashkin et al., 2001).

In contrast to the other lipid metabolites, hepatic diacylglycerol content was the most consistent predictor of hepatic insulin sensitivity in high-fat-diet-fed *mtGPAT1*$^{-/-}$ mice. Diacylglycerol has been shown to activate an array of PKC isoenzymes that are capable of inhibiting insulin receptor tyrosine kinase activity by initiation of serine/threonine phosphorylation of the insulin receptor or insulin receptor substrate (Considine et al., 1995; Ikeda et al., 2001; Nishizuka, 2003; Samuel et al., 2004; Takai et al., 1979; Yu et al., 2002). A possible role for decreased diacylglycerol levels in preserving hepatic insulin sensitivity is supported by the observation of decreased hepatic PKCϵ activation in high-fat-fed *mtGPAT1*$^{-/-}$ mice (Figure 4C).

The role of triacylglycerol in the genesis of insulin resistance is unclear. While intramyocellular lipid content is an excellent marker for insulin resistance in skeletal muscle of sedentary individuals (Krssak et al., 1999; Perseghin et al., 1999; Petersen et al., 2004), recent animal studies have been able to dissociate intramuscular triacylglycerol content from fat-induced insulin resistance in skeletal muscle (Yu et al., 2002). Most studies to

date both in humans and animal models, including the present study, have found a strong relationship between hepatic triacylglycerol content and hepatic insulin sensitivity (Bajaj et al., 2004; Chou et al., 2002; Jucker et al., 1999; Petersen et al., 2005; Samuel et al., 2004; Voshol et al., 2003). Whether hepatic triacylglycerol is the actual trigger or merely a marker for fat-induced hepatic insulin resistance remains to be determined. A number of mouse models lacking enzymes that are involved in triacylglycerol synthesis and cause alterations in lipid homeostasis have been generated in the past few years. Mice deficient in acyl-CoA:diacylglycerol transferase 1 (DGAT1), catalyzing the final step in the glycerol 3-phosphate pathway, share several phenotypic similarities with *mtGPAT1*$^{-/-}$ mice (Chen et al., 2002; Smith et al., 2000). *DGAT1*$^{-/-}$ mice are lean, have smaller fat pads, and lack alterations in plasma glucose, insulin, and fatty-acid concentrations. But in contrast to *mtGPAT1*$^{-/-}$ mice, *DGAT1*$^{-/-}$ mice are hypoleptinemic, hypersensitive to leptin and insulin, normotriglyceridemic, display a markedly lower triacylglycerol content in skeletal muscle but not liver, and are resistant to diet-induced obesity through a mechanism involving increased energy expenditure and activity (Chen et al., 2002; Smith et al., 2000). DGAT2, the second characterized DGAT isoenzyme, is essential for triacylglycerol synthesis. *DGAT2*$^{-/-}$ mice die early in the postnatal period probably due to an impaired permeability barrier function in the skin and from a lack of key substrates for energy metabolism and triacylglycerol synthesis during development (Stone et al., 2004).

It has been demonstrated previously that *mtGPAT1* overexpression in hepatocytes reduces the oxidation of radiolabeled palmitic and oleic acid (Lewin et al., 2005, Lindén et al., 2004). As rates of fatty-acid oxidation and ketogenesis usually correlate, increased fasting plasma β-hydroxybutyrate concentrations in high-fat-diet-fed *mtGPAT1*$^{-/-}$ mice likely reflect an increase in fatty-acid β-oxidation. Stearoyl-CoA desaturase (SCD) catalyzes the rate-limiting step in the biosynthesis of monounsaturated fatty acids. *SCD*$^{-/-}$ mice display increased fatty-acid β-oxidation rates likely involving AMPK-induced inactivation of acetyl-CoA carboxylase and subsequent intracellular decreases in the carnitine palmitoyltransferase 1 (CPT-1) inhibitor malonyl-CoA (Dobrzyn et al., 2004). In contrast to *SCD*$^{-/-}$ mice, the present findings suggest that different regulatory mechanisms modulate hepatic fatty-acid β-oxidation in *mtGPAT1*$^{-/-}$ mice since the hepatic content of pAMPK protein, pACC protein, and malonyl-CoA were similar in *mtGPAT1*$^{-/-}$ and wt mice.

Another regulator of hepatic fatty-acid oxidation is the nuclear transcription peroxisome proliferator-activated receptor α (PPARα) that once activated induces gene transcription of an array of enzymes involved in mitochondrial and peroxisomal β-oxidation and microsomal ω-oxidation (Bardot et al., 1993; Bars et al., 1993; Besnard et al., 1993; Hijikata et al., 1990; Osumi et al., 1991). The n-3 fatty acids C20:5n-3 or C22:6n-3 have been shown to serve as PPARα ligands and promote hepatic peroxisome proliferation in vivo (Forman et al., 1997; Hashimoto et al., 1999; Neschen et al., 2002). However, despite an increase in hepatic n-3 fatty-acid-derived CoA species in *mtGPAT1*$^{-/-}$ mice neither the expression of PPARα or of the PPARα responsive gene peroxisomal acyl-CoA oxidase 1 differed between genotypes.

In conclusion, *mtGPAT1*$^{-/-}$ mice were protected from high-fat-diet-induced hepatosteatosis and hepatic insulin resistance. Consistent with mtGPAT1's tissue distribution, this protection from fat-induced insulin resistance was restricted to liver and white adipose tissue but not skeletal muscle. In *mtGPAT1*$^{-/-}$ mice, preservation of hepatic insulin sensitivity in vivo correlated with enhanced insulin signaling on the cellular level but was not related to increased intrahepatic acyl-CoA concentrations, implying that acyl-CoA's do not mediate fat-induced hepatic insulin resistance. In contrast, protection of fat-induced hepatic insulin resistance was correlated with reduced fasting concentrations of diacylglycerol, further implicating this metabolite as a potentially important mediator of fat-induced hepatic insulin resistance. These data also suggest that mtGPAT1 might be a potent therapeutic target to treat hepatic steatosis and hepatic insulin resistance.

Experimental procedures

Animals and dietary treatment

Male, age-matched mice deficient in *mtGPAT* (*mtGPAT1*$^{-/-}$, C57BL/6J genetic background, F_6 generation; Hammond et al., 2002) and wild-type (wt) mice were singly housed, and in order to minimize stress to the animals, experiments were carried out in several separate but identically treated groups of mice. While on a control diet (Teklad LM-485, 7912, 5% wt/wt soybean oil, Harlan, Madison, Wisconsin), a first set of intraperitoneal glucose tolerance tests (1 g glucose/kg) was performed. At an age of 14–21 weeks mice, were started on a high-fat safflower oil based diet (27% wt/wt safflower oil, 59% fat-derived calories, 5.18 kcal/g) and fed for 3 weeks. The safflower oil diet (#112245, Dyets, Bethlehem, Pennsylvania) was supplemented with minerals and vitamins (#210025, #310025). Food was exchanged every third day and individual food consumption rates, body weight gain, and body composition using in vivo NMR-spectroscopy (Minispec MQ10 analyzer, Bruker Optics Inc, Billerica, Massachusetts) were measured at baseline and weekly throughout dietary intervention. After 1 week of high-fat feeding, a second set of intraperitoneal glucose tolerance tests (1 g glucose/kg) was carried out. From further mouse batches, plasma and tissue samples under basal or after 20 min insulin-stimulated conditions (intraperitoneal 0.5 mU/kg) were harvested under isoflurane anesthesia. Fat absorption from a semi-synthetic low-fat or high-fat diet (7% or 27% wt/wt safflower oil) supplemented with 5% sucrose polybehenate, a marker for the intestinal transit of dietary fat, was assessed according to techniques described earlier (Jandacek et al., 2004). Fat absorption was calculated from the ratios of behenic acid to linolenic acid in diet and feces collected on day two analyzed by gas chromatography of fatty-acid methyl esters. All experiments were carried out in 16 hr food-deprived mice, except intraperitoneal glucose tolerance tests after 1 week of high-fat feeding, where food was removed 6 hr prior to the experiment. All procedures were approved by the Yale University Animal Care and Use Committee.

Euglycemic-hyperinsulinemic glucose clamp experiments

One week prior to experiments, an intravenous silicone catheter was inserted into the right jugular vein under ketamine/xylazine anesthesia (intraperitoneal 80/10 mg/kg body weight). On the experimental day, the subcutaneously located sealed catheter-tip was accessible via a small interscapular skin incision. Conscious mice were placed in restraining tubes, their tails secured with tape. In vivo experiments lasted for 240 min and consisted of a 120 min basal period directly followed by a 120 min euglycemic-hyperinsulinemic clamp as previously described (Ren et al., 1995). During the basal period, a prime-continuous [3-^{3}H]glucose infusion (10 μCi bolus, 0.1 μCi/min) was started and continued to determine rates of whole-body glucose turnover. After the 120 min basal infusion period, a primed-continuous insulin infusion (2.5 mU/kg*min^{-1}; Humulin, Eli Lilly, Indianapolis, Indiana) was started at time 0 min, raising insulin levels within a physiologic range (control diet: 75 ± 2, n = 4 versus 74 ± 5, n = 5 μU/ml insulin in wt, p = 0.9; high-fat diet: 67 ± 3, n = 7 versus 66 ± 2, n = 8 μU/ml insulin in wt, p = 0.8). "Steady-state" conditions for plasma glucose concentration (control diet: 118 ± 4, n = 4 versus 114 ± 9, n = 5 mg/dl glucose in wt, p = 0.7; high-fat diet: 105 ± 5, n = 7 versus 117 ± 4, n = 8

mg/dl glucose in wt, p = 0.08) and specific activity were achieved within 70 min, and a single 2-deoxy-D-[1-^{14}C]glucose (2-[^{14}C]DG) injection was administered at time 75 min. To determine plasma [3-^{3}H]glucose, $^{3}H_2O$, and 2-[^{14}C]DG concentrations, blood samples were collected at time 80, 85, 90, 100, 110, and 120 min of the clamp and for measurement of basal [3-^{3}H]glucose concentrations in the final 10 min of the basal period. A plasma sample for determination of basal insulin levels was obtained during the final 10 min of the basal period and for steady-state insulin levels at minute 120 of the clamp. All infusions were performed with microdialysis pumps (CMA/Microdialysis, North Chelmsford, Massachusetts) and radioisotopes purchased from Perkin Elmer Life Sciences (Boston, Massachusetts) and American Radiolabeled Chemicals (St. Louis, Missouri). At the end of the experiment, animals were anesthetized with ketamine/xylazine (intravenous 80/10 mg/kg) and liver, epididymal white adipose tissue, and *M. gastrocnemius* including *M. soleus* were immediately freeze-clamped and stored at −80°C until further analysis.

Calculations

The rate of whole-body glucose turnover was calculated as the ratio of [3-^{3}H]glucose infusion rate (dpm/min) and plasma [3-^{3}H]glucose-specific activity (dpm/min*μmol) during steady state. Hepatic [3-^{3}H]glucose production (HGP) was determined by subtracting the steady-state glucose infusion rate (GINF) from the rate of glucose whole-body turnover. 2-[^{14}C]DG uptake in gastrocnemius muscle and epididymal white adipose tissue were calculated from plasma 2-[^{14}C]DG AUC at minute 80, 85, 90, 100, 110, to 120 and tissue 2-[^{14}C]DG-6-phosphate content as described previously (Ohshima et al., 1984).

Assays from plasma

Glucose concentration was determined with a Glucose Analyzer (Beckman, Fullerton, California), triacylglycerol, nonesterified fatty-acid, β-hydroxybutyrate, cholesterol, and HDL cholesterol levels with a Cobas Mira Analyzer (Roche Diagnostics). Plasma insulin, glucagon, leptin, adiponectin (Linco Research, St. Charles, Missouri), and corticosterone (ICN, Costa Mesa, California) were measured via radioimmunoassay. Plasma [3-^{3}H]glucose and 2-[^{14}C]DG was determined from deproteinized plasma samples (Somogyi filtrates) after $^{3}H_2O$ was completely evaporated from the supernatant using a Liquid Scintillation Counter (Ultima Gold; Packard Instrument Co, Meriden, Connecticut).

Tissue 2-[^{14}C]DG-6P enrichment

2-[^{14}C]DG injected during steady-state conditions of euglycemic-hyperinsulinemic clamp experiments resulted in intracellular accumulation of 2-[^{14}C]DG-6P in tissue. 2-[^{14}C]DG-6P in gastrocnemius muscle and epididymal white adipose tissue homogenates was separated from 2-[^{14}C]DG using ion-exchange columns (Poly-Prep #731-6211; Bio-Rad, Hercules, California) according to a technique previously described (Griffin et al., 1999).

Tissue lipid metabolites

The extraction procedure for acyl-CoA species was adapted from methods described previously (Deutsch et al., 1994; Neschen et al., 2002). Approximately 100 mg of liver or skeletal muscle (*M. quadriceps*) tissue were homogenized with C17:0 acyl-CoA-ester internal standard. After purification using Oligonucleotide Purification Cartridges (Applied Biosystems, Foster City, California) and a drying step, medium, long-chain, and very long-chain acyl-CoA fractions were dissolved in methanol/H_2O (1:1, v/v).

For lysophosphatidic and phosphatidic acid measurements, approximately 100 mg of liver tissue was homogenized in chloroform/methanol (1:1 vol/vol) with 1 nmol/l C17-lysophosphatidic acid internal standard. After phase separation with dH_2O, samples were homogenized, centrifuged, and the methanol/water phase collected. The supernatant was applied to conditioned Waters Oasis MAX extraction cartridges (Waters Corporation, Milford, Massachusetts). After a washing step, lysophosphatidic and phosphatidic acid species were eluted using methanol.

The extraction procedure for diacylglycerol was adapted from methods described previously (Pacheco et al., 1998). Approximately 100 mg of liver tissue was homogenized in ice-cold chloroform/methanol (2:1 vol/vol) containing 0.01% butylated hydroxytoluene and the internal standards 1,3-dipenta decanoin and 1,2,3-triheptadecanoate. Organic and aqueous phase were separated adding chloroform and H_2O. After centrifugation, the organic layer was collected, dried under nitrogen flow, and reconstituted with hexane/methylene chloride/ether (95/4.5/0.5 vol/vol/vol). Diacylglycerol was separated from triacylglycerol using preconditioned columns (Waters Sep-Pak Cartridge WAT020845, Milford, Massachusetts) and eluted with hexane/ethyl acetate (85/15 vol/vol) under a low negative pressure.

Lipid metabolite extracts were subjected to LC/MS/MS analysis. A turbo ionspray source was interfaced with an API 3000 tandem mass spectrometer (Applied Biosystems, Foster City, California) in conjunction with two Perkin Elmer 200 Series micro pumps and a 200 Series autosampler (Perkin Elmer, Norwalk, Connecticut). Total acyl-CoA, lysophosphatidic acid, phosphatidic acid, and diacylglycerol content were expressed as the sum of individual species.

Tissue triacylglycerol content

The extraction procedure for tissue triacylglycerol was adapted from methods described previously (Frayn and Maycock, 1980; Neschen et al., 2002). Triacylglycerol content of each sample was measured in duplicate after evaporation of the organic solvent using an enzymatic method (Sigma Diagnostics, St. Louis, Missouri).

Tissue malonyl-CoA content

Approximately 100 mg of liver tissue were homogenized in ice-cold 10% trichloroacetic acid with the addition of $^{13}C_3$-malonyl-CoA internal standard. After centrifugation, the supernatant was applied to a preconditioned cartridge (C18 Waters Sep-Pak Cartridge WAT036905, Milford, Massachusetts) and following washing steps eluted with 65% ethanol containing 0.1 M NH_4-acetate and 50% methanol. Samples were lyophilized and redissolved in water. Malonyl-CoA and acetyl-CoA were separated by HPLC with isocratic 15% methanol and 10 mM ammonium acetate and measured using LC/MS/MS analysis.

Western blot analysis

Proteins extracted from freeze-clamped basal liver tissue were resolved by electrophoresis and electrotransferred onto PVDF membranes (Amersham Pharmacia Biotech Inc.). Membranes were immunoblotted with antibodies recognizing phosphorylation of AMP-activated protein kinase α-1/α-2 at Thr^{172}, phosphorylation of acetyl-CoA carboxylase α/β at Ser^{97}, or phosphorylation of glycogen synthase kinase-3 α/β at Ser^{21} and Ser^{9} (Cell Signaling Technology, Beverly, Massachusetts).

PKCε membrane translocation assays were performed according to methods previously described (Qu et al., 1999; Donnelly et al., 1994). Briefly, 50 μg of crude membrane and cytosol protein extracts were resolved by SDS-PAGE using an 8% gel and electrotransferred onto PVDF. Membranes were immunoblotted with a rabbit anti-peptide antibody against PKCε (Santa Cruz Biotechnology, Santa Cruz, California) diluted 1:100 in rinsing solution. PKCε translocation was expressed as the ratio of arbitrary units of membrane bands over cytosol bands.

Protein bands were quantitated using a Bio-Rad Chemidoc SRX and Quantity One Software (Biorad, Hercules, California).

Liver IRS2-associated PI3K and Akt2 activity

IRS2-associated PI3K and Akt2 activity were assessed in 4 mg protein extracts from livers harvested after short-term insulin stimulation. Assays were performed according to methods previously described (Alessi et al., 1996; Folli et al., 1992). Primary antibodies used for these experiments were rabbit polyclonal IgG. All materials were obtained from Upstate (Charlottesville, Virginia).

Quantitative RT-PCR-based gene expression analysis

RNA was isolated from post-clamp livers using a commercially available kit (Qiagen RNeasy Kit, Qiagen Inc, Valencia, California) in combination with DNase digest treatment. After 1.5 μg of total RNA were reverse transcribed (Stratagene, La Jolla, California) with an oligo-prime, PCR was performed with a DNA Engine Opticon 2 System (MJ Research, Boston, Massachusetts) using SYBR green QPCR dye kit (Stratagene). The following primers were used: phosphoenolpyruvate carboxykinase (PEPCK): 5′ ACC TCC TGG AAG AAC AAG GA 3′ (F) and 5′ CTC ATG GCT GCT CCT ACA AA 3′ (R); sterol regulatory-element binding protein 1c (SREBP1c): 5′ CAT GGA TTG CAC ATT TGA AGA 3′ (F) and 5′ CTG TGT CCC CTG TCT CAC C 3′

(R); peroxisome proliferator-activated receptor α: 5′ TAT TCG GCT GAA GCT GGT GTA CC 3′ (F) and 5′ CTG GCA TTT GTT CCG GTT CT 3′ (R); peroxisomal acyl-CoA oxidase 1: 5′ AGC TCC GAT CAG CCA GAC AT 3′ (F) and 5′ TTC TTG AAA CAG AGC CCA GAA TG 3′ (R); long-chain acyl-CoA dehydrogenase: 5′ CAC TCA GAT ATT GTC ATG CCC T 3′ (F) and 5′ TCC ATT GAG AAT CCA ATC ACT C 3′ (R); very long-chain acyl-CoA dehydrogenase: 5′ CCT GAA GAA TCC TTT TGG AAA C 3′ (F) and 5′ CTT TCT TGT GTT TCA CCA GCT T 3′ (R); 18S rRNA: 5′ TTC CGA TAA CGA ACG AGA CTC T 3′ (F) and 5′ TGG CTG AAC GCC ACT TGT C 3′ (R). Product specificity was verified by running products on an agarose gel. Messenger RNA levels (ΔC_T values), normalized to 18S rRNA, were expressed using the comparative method. 18S rRNA levels showed no statistical difference between genotypes.

Statistical analysis

All data are expressed as mean ± SEM. Statistical analyses were made using a two-tailed Student's t test, and for all hypotheses, the significance level was 0.05.

Supplemental data

Supplemental data include one figure and are available with this article online at http://www.cellmetabolism.org/cgi/content/full/2/1/55/DC1/.

Acknowledgments

We thank Aida Grossmann, Yanna Kosover, and Saki Sono for their excellent technical assistance. We thank Dr. Jandacek and Dr. Tso from the University of Cincinnati Mouse Metabolic Phenotyping Center for their scientific expertise and technical help in the lipid absorption studies. This work was supported by grants from the National Institutes of Health: R01 DK-40936 (G.I.S.), U24 DK-59635 (G.I.S.), R01 DK-56598 (R.A.C.), and F31 GM20920 (L.E.H.). G.I.S. is the recipient of a Distinguished Clinical Scientist Award from the American Diabetes Association and an Investigator of the Howard Hughes Medical Institute.

Received: November 30, 2004
Revised: May 10, 2005
Accepted: June 22, 2005
Published: July 19, 2005

References

Alessi, D.R., Caudwell, F.B., Andjelkovic, M., Hemmings, B.A., and Cohen, P. (1996). Molecular basis for the substrate specificity of protein kinase B; comparison with MAPKAP kinase-1 and p70 S6 kinase. FEBS Lett. *399*, 333–338.

Bajaj, M., Suraamornkul, S., Piper, P., Hardies, L.J., Glass, L., Cersosimo, E., Pratipanawatr, T., Miyazaki, Y., and DeFronzo, R.A. (2004). Decreased plasma adiponectin concentrations are closely related to hepatic fat content and hepatic insulin resistance in pioglitazone-treated type 2 diabetic patients. J. Clin. Endocrinol. Metab. *89*, 200–206.

Bardot, O., Aldridge, T.C., and Green, S. (1993). PPAR-RXR heterodimer activates a peroxisome proliferator response element upstream of the bifunctional enzyme gene. Biochem. Biophys. Res. Commun. *192*, 37–45.

Bars, R.G., Bell, D.R., and Elcombe, C.R. (1993). Induction of cytochrome P450 and peroxisomal enzymes by clofibric acid in vivo and in vitro. Biochem. Pharmacol. *45*, 2045–2053.

Besnard, P., Mallordy, A., and Carlier, H. (1993). Transcriptional induction of the fatty acid binding protein gene in mouse liver by bezafibrate. FEBS Lett. *327*, 219–223.

Bhat, B.G., Wang, P., Kim, J.-H., Black, T.M., Lewin, T.M., Fiedorek, T.M., and Coleman, R.A. (1999). Rat hepatic sn-glycerol-3-phosphate acyltransferase: Molecular cloning and characterization of the cDNA and expressed protein. Biochim. Biophys. Acta *1439*, 415–423.

Chen, M.T., Kaufman, L.N., Spennetta, T., and Shrago, E. (1992). Effects of high fat-feeding to rats on the interrelationship of body weight, plasma insulin, and fatty acyl-coenzyme A esters in liver and skeletal muscle. Metabolism *41*, 564–569.

Chen, H.C., Smith, S.J., Ladha, Z., Jensen, D.R., Ferreira, L.D., Pulawa, L.K., McGuire, J.G., Pitas, R.E., Eckel, R.H., and Farese, R.V., Jr. (2002). Increased insulin and leptin sensitivity in mice lacking acyl CoA:diacylglycerol acyltransferase 1. J. Clin. Invest. *109*, 1049–1055.

Chou, C.J., Haluzik, M., Gregory, C., Dietz, K.R., Vinson, C., Gavrilova, O., and Reitman, M.L. (2002). WY14,643, a peroxisome proliferator-activated receptor alpha (PPARalpha) agonist, improves hepatic and muscle steatosis and reverses insulin resistance in lipoatrophic A-ZIP/F-1 mice. J. Biol. Chem. *277*, 24484–24489.

Coleman, R.A., and Haynes, E.B. (1983). Differentiation of microsomal from lysosomal triacylglycerol lipase activities in rat liver. Biochim. Biophys. Acta *751*, 230–240.

Coleman, R.A., and Lee, D.P. (2004). Enzymes of triacylglycerol synthesis and their regulation. Prog. Lipid Res. *43*, 134–176.

Coleman, R.A., Lewin, T.M., and Muoio, D.M. (2000). Physiological and nutritional regulation of enzymes of triacylglycerol synthesis. Annu. Rev. Nutr. *20*, 77–103.

Considine, R.V., Nyce, M.R., Allen, L.E., Morales, L.M., Triester, S., Serrano, J., Colberg, J., Lanza-Jacoby, S., and Caro, J.F. (1995). Protein kinase C is increased in the liver of humans and rats with non-insulin-dependent diabetes mellitus: an alteration not due to hyperglycemia. J. Clin. Invest. *95*, 2938–2944.

Deutsch, J., Grange, E., Rapoport, S.I., and Purdon, A.D. (1994). Isolation and quantitation of long-chain acyl-coenzyme A esters in brain tissue by solid-phase extraction. Anal. Biochem. *220*, 321–323.

Dobrzyn, P., Dobrzyn, A., Miyazaki, M., Cohen, P., Asilmaz, E., Hardie, D.G., Friedman, J.M., and Ntambi, J.M. (2004). Stearoyl-CoA desaturase 1 deficiency increases fatty acid oxidation by activating AMP-activated protein kinase in liver. Proc. Natl. Acad. Sci. USA *101*, 6409–6414.

Donnelly, R., Reed, M.J., Azhar, S., and Reaven, G.M. (1994). Expression of the major isoenzyme of protein kinase-C in skeletal muscle, nPKC theta, varies with muscle type and in response to fructose-induced insulin resistance. Endocrinology *135*, 2369–2374.

Fang, X., Yu, S., Tanyi, J.L., Lu, Y., Woodgett, J.R., and Mills, G.B. (2002). Convergence of multiple signaling cascades at glycogen synthase kinase 3: Edg receptor-mediated phosphorylation and inactivation by lysophosphatidic acid through a protein kinase C-dependent intracellular pathway. Mol. Cell. Biol. *22*, 2099–2110.

Folli, F., Saad, M.J., Backer, J.M., and Kahn, C.R. (1992). Insulin stimulation of phosphatidylinositol 3-kinase activity and association with insulin receptor substrate 1 in liver and muscle of the intact rat. J. Biol. Chem. *267*, 22171–22177.

Forman, B.M., Chen, J., and Evans, R.M. (1997). Hypolipidemic drugs, polyunsaturated fatty acids, and eicosanoids are ligands for peroxisome proliferators-activated receptors α and δ. Proc. Natl. Acad. Sci. USA *94*, 4312–4317.

Frayn, K.N., and Maycock, P.F. (1980). Skeletal muscle triacylglycerol in the rat: methods for sampling and measurement, and studies of biological variability. J. Lipid Res. *21*, 139–144.

Griffin, M.E., Marcucci, M.J., Cline, G.W., Bell, K., Barucci, N., Lee, D., Goodyear, L.J., Kraegen, E.W., White, M.F., and Shulman, G.I. (1999). Free fatty acid-induced insulin resistance is associated with activation of protein kinase C theta and alterations in the insulin signaling cascade. Diabetes *48*, 1270–1274.

Hammond, L.E., Gallagher, P.A., Wang, S., Hiller, S., Kluckman, K.D., Posey-Marcos, E.L., Maeda, N., and Coleman, R.A. (2002). Mitochondrial glycerol-3-phosphate acyltransferase-deficient mice have reduced weight and liver triacylglycerol content and altered glycerolipid fatty acid composition. Mol. Cell. Biol. *22*, 8204–8214.

Hashimoto, T., Fujita, T., Usuda, N., Cook, W., Qi, C., Peters, J.M., Gonza-

lez, F.J., Yeldandi, A.V., Rao, M.S., and Reddy, J.K. (1999). Peroxisomal and mitochondrial fatty acid beta-oxidation in mice nullizygous for both peroxisome proliferator-activated receptor alpha and peroxisomal fatty acyl-CoA oxidase. Genotype correlation with fatty liver phenotype. J. Biol. Chem. *274*, 19228–19236.

Hegarty, B.D., Furler, S.M., Ye, J., Cooney, G.J., and Kraegen, E.W. (2003). The role of intramuscular lipid in insulin resistance. Acta Physiol. Scand. *178*, 373–383.

Hijikata, M., Wen, J.K., Osumi, T., and Hashimoto, T. (1990). Rat peroxisomal 3-ketoacyl-CoA thiolase gene: occurrence of two closely related but differentially regulated genes. J. Biol. Chem. *265*, 4600–4606.

Igal, R.A., Wang, S., Gonzalez-Baró, M., and Coleman, R.A. (2001). Mitochondrial glycerol phosphate acyltransferase directs cellular triacylglycerol synthesis. J. Biol. Chem. *276*, 42205–42212.

Ikeda, Y., Olsen, G.S., Ziv, E., Hansen, L.L., Busch, A.K., Hansen, B.F., Shafrir, E., and Mosthaf-Seedorf, L. (2001). Cellular mechanism of nutritionally induced insulin resistance in Psammomys obesus: overexpression of protein kinase C epsilon in skeletal muscle precedes the onset of hyperinsulinemia and hyperglycemia. Diabetes *50*, 584–592.

Jandacek, R.J., Heubi, J.E., and Tso, P. (2004). A novel, noninvasive method for the measurement of intestinal fat absorption. Gastroenterology *127*, 139–144.

Jucker, B.M., Cline, G.W., Barucci, N., and Shulman, G.I. (1999). Differential effects of safflower oil versus fish oil feeding on insulin-stimulated glycogen synthesis, glycolysis, and pyruvate dehydrogenase flux in skeletal muscle: a ^{13}C nuclear magnetic resonance study. Diabetes *48*, 134–140.

Kraegen, E.W., Cooney, G.J., Ye, J.M., Thompson, A.L., and Furler, S.M. (2001). The role of lipids in the pathogenesis of muscle insulin resistance and beta cell failure in type II diabetes and obesity. Exp. Clin. Endocrinol. Diabetes *109*, S189–S201.

Krssak, M., Falk Petersen, K., Dresner, A., DiPietro, L., Vogel, S.M., Rothman, D.L., Roden, M., and Shulman, G.I. (1999). Intramyocellular lipid concentrations are correlated with insulin sensitivity in humans: a ^{1}H NMR spectroscopy study. Diabetologia *42*, 113–116.

Lee, R.G. (1989). Nonalcoholic steatohepatitis: a study in 49 patients. Hum. Pathol. *20*, 594–598.

Lewin, T.M., Granger, D.A., Kim, J.-H., and Coleman, R.A. (2001). Regulation of mitochondrial sn-glycerol-3-phophate acyltransferase activity: response to feeding status is unique in various rat tissues and is discordant with protein expression. Arch. Biochem. Biophys. *396*, 119–127.

Lewin, T.M., Schwerbrock, N.M., Lee, D.P., and Coleman, R.A. (2004). Identification of a new glycerol-3-phosphate acyltransferase isoenzyme, mtGPAT2, in mitochondria. J. Biol. Chem. *279*, 13488–13495.

Lewin, T.M., Wang, S., Nagle, C.A., Van Horn, C.G., and Coleman, R.A. (2005). Mitochondrial glycerol-3-phosphate acyltransferase-1 directs the metabolic fate of exogenous fatty acids in hepatocytes. Am. J. Physiol. Endocrinol. Metab. *288*, E835–E844.

Lindén, D., William-Olsson, L., Rhedin, M., Asztély, A.K., Clapham, J.C., and Schreyer, S. (2004). Overexpression of mitochondrial GPAT in rat hepatocytes leads to decreased fatty acid oxidation and increased glycerolipid biosynthesis. J. Lipid Res. *45*, 1279–1288.

Marchesini, G., Brizi, M., Morselli-Labate, A.M., Bianchi, G., Bugianesi, E., McCullough, A.J., Forlani, G., and Melchionda, N. (1999). Association of nonalcoholic fatty liver disease with insulin resistance. Am. J. Med. *197*, 450–455.

Mayerson, A.B., Hundal, R.S., Dufour, S., Lebon, V., Befroy, D., Cline, G.W., Enocksson, S., Inzucchi, S.E., Shulman, G.I., and Petersen, K.F. (2002). The effects of rosiglitazone on insulin sensitivity, lipolysis, and hepatic and skeletal muscle triglyceride content in patients with type 2 diabetes. Diabetes *51*, 797–802.

Monroy, G., Rola, F.H., and Pullman, M.E. (1972). A substrate and position-specific acylation of sn-glycerol 3-phosphate by rat liver mitochondria. J. Biol. Chem. *247*, 6884–6894.

Neschen, S., Moore, I., Regittnig, W., Yu, C.L., Wang, Y., Pypaert, M., Petersen, K.F., and Shulman, G.I. (2002). Contrasting effects of fish oil and safflower oil on hepatic peroxisomal and tissue lipid content. Am. J. Physiol. Endocrinol. Metab. *282*, E395–E401.

Nishizuka, Y. (2003). Discovery and prospect of protein kinase C research: epilogue. J. Biochem. (Tokyo) *133*, 155–158.

Ohshima, K., Shargill, N.S., Chan, T.M., and Bray, G.A. (1984). Adrenalectomy reverses insulin resistance in muscle from obese (ob/ob) mice. Am. J. Physiol. *246*, E193–E197.

Osumi, T., Wen, K.-K., and Hashimoto, T. (1991). Two cis-acting regulatory sequences in the peroxisome proliferator-responsive enhancer region of rat acyl-CoA oxidase gene. Biochem. Biophys. Res. Commun. *175*, 866–871.

Pacheco, Y.M., Perez-Camino, M.C., Cert, A., Montero, E., and Ruiz-Gutierrez, V. (1998). Determination of the molecular species composition of diacylglycerols in human adipose tissue by solid-phase extraction and gas chromatography on a polar phase. J. Chromatogr. B Biomed. Sci. Appl. *714*, 127–132.

Paulauskis, J.D., and Sul, H.S. (1988). Cloning and expression of mouse fatty acid synthase and other specific mRNAs: developmental and hormonal regulation in 3T3–L1 cells. J. Biol. Chem. *263*, 7049–7054.

Perseghin, G., Scifo, P., De Cobelli, F., Pagliato, E., Battezzati, A., Arcelloni, C., Vanzulli, A., Testolin, G., Pozza, G., Del Maschio, A., and Luzi, L. (1999). Intramyocellular triglyceride content is a determinant of in vivo insulin resistance in humans: a ^{1}H-^{13}C nuclear magnetic resonance spectroscopy assessment in offspring of type 2 diabetic parents. Diabetes *48*, 1600–1606.

Petersen, K.F., Oral, E.A., Dufour, S., Befroy, D., Ariyan, C., Yu, C., Cline, G.W., DePaoli, A.M., Taylor, S.I., Gorden, P., and Shulman, G.I. (2002). Leptin reverses insulin resistance and hepatic steatosis in patients with severe lipodystrophy. J. Clin. Invest. *109*, 1345–1350.

Petersen, K.F., Dufour, S., Befroy, D., Garcia, R., and Shulman, G.I. (2004). Impaired mitochondrial activity in the insulin-resistant offspring of patients with type 2 diabetes. N. Engl. J. Med. *350*, 664–671.

Petersen, K.F., Dufour, S., Befroy, D., Lehrke, M., Hendler, R.E., and Shulman, G.I. (2005). Reversal of nonalcoholic hepatic steatosis, hepatic insulin resistance, and hyperglycemia by moderate weight reduction in patients with type 2 diabetes. Diabetes *54*, 603–608.

Pietilainen, K.H., Rissanen, A., Kaprio, J., Makimattila, S., Hakkinen, A.M., Westerbacka, J., Sutinen, J., Vehkavaara, S., and Yki-Jarvinen, H. (2005). Acquired obesity is associated with increased liver fat, intra-abdominal fat, and insulin resistance in young adult monozygotic twins. Am. J. Physiol. Endocrinol. Metab. *288*, E768–E774.

Qu, X., Seale, J.P., and Donnelly, R. (1999). Tissue and isoform-selective activation of protein kinase C in insulin-resistant obese Zucker rats — effects of feeding.. J. Endocrinology *162*, 207–214.

Ren, J.M., Marshall, B.A., Mueckler, M.M., McCaleb, M., Amatruda, J.M., and Shulman, G.I. (1995). Overexpression of Glut4 protein in muscle increases basal and insulin-stimulated whole body glucose disposal in conscious mice. J. Clin. Invest. *95*, 429–432.

Samuel, V.T., Liu, Z.X., Qu, X., Elder, B.D., Bilz, S., Befroy, D., Romanelli, A.J., and Shulman, G.I. (2004). Mechanism of hepatic insulin resistance in non-alcoholic fatty liver disease. J. Biol. Chem. *279*, 32345–32353.

Shashkin, P.N., Wasner, H.K., Ortmeyer, H.K., and Hansen, B.C. (2001). Prostaglandylinositol cyclic phosphate (cPIP): a novel second messenger of insulin action. Comparative analysis of two kinds of "insulin mediators." Diabetes Metab. Res. Rev. *17*, 273–284.

Shin, D.-H., Paulauskis, J.D., Moustaid, N., and Sul, H.S. (1991). Transcriptional regulation of p90 with sequence homology to Escherichia coli glycerol-3-phosphate acyltransferase. J. Biol. Chem. *266*, 23834–23839.

Shulman, G.I. (2000). Cellular mechanisms of insulin resistance. J. Clin. Invest. *106*, 171–176.

Smith, S.J., Cases, S., Jensen, D.R., Chen, H.C., Sande, E., Tow, B., Sanan, D.A., Raber, J., Eckel, R.H., and Farese, R.V., Jr. (2000). Obesity resistance and multiple mechanisms of triglyceride synthesis in mice lacking Dgat. Nat. Genet. *25*, 87–90.

Stone, S.J., Myers, H.M., Watkins, S.M., Brown, B.E., Feingold, K.R., Elias, P.M., and Farese, R.V., Jr. (2004). Lipopenia and skin barrier abnormalities in DGAT2-deficient mice. J. Biol. Chem. *279*, 11767–11776.

Takai, Y., Kishimoto, A., Kikkawa, U., Mori, T., and Nishizuka, Y. (1979). Unsaturated diacylglycerol as a possible messenger for the activation of calcium-activated, phospholipid-dependent protein kinase system. Biochem. Biophys. Res. Commun. *91*, 1218–1224.

Voshol, P.J., Haemmerle, G., Ouwens, D.M., Zimmermann, R., Zechner, R., Teusink, B., Maassen, J.A., Havekes, L.M., and Romijn, J.A. (2003). Increased hepatic insulin sensitivity together with decreased hepatic triglyceride stores in hormone-sensitive lipase-deficient mice. Endocrinology *144*, 3456–3462.

Yet, S.F., Lee, S., Hahm, Y.T., and Sul, H.S. (1993). Expression and identification of p90 as the murine mitochondrial glycerol-3-phosphate acyltransferase. Biochemistry *32*, 9486–9491.

Yu, C., Chen, Y., Cline, G.W., Zhang, D., Zong, H., Wang, Y., Bergeron, R., Kim, J.K., Cushman, S.W., Cooney, G.J., et al. (2002). Mechanism by which fatty acids inhibit insulin activation of insulin receptor substrate-1 (IRS-1)-associated phosphatidylinositol 3-kinase activity in muscle. J. Biol. Chem. *277*, 50230–50236.